NUMERICAL NEAR-FIELD SIMULATIONS OF LOW BOOM AIRCRAFT CONCEPTS

J. Kirz, German Aerospace Center (DLR), Institute of Aerodynamics and Flow Technology, Lilienthalplatz 7, 38108 Braunschweig, Germany

Abstract

This paper presents the setup of the DLR TAU code for sonic boom near-field simulations and results obtained for the low-boom geometries developed within the EC project RUMBLE. A process for surrogate-based low-boom low-drag fuselage design based on a near-field target pressure signature is described. The focus of the paper is the robust parameterization of the fuselage geometry to prevent the generation of irregular shapes as well as the modular grid generation approach that significantly reduces the time to generate the grids. The numerical results of four RUMBLE milestone shape evolutions with flow through nacelles are presented and geometrical influences on the near-field pressure signatures are analyzed. It is shown that the pressure signatures for shape derivatives with powered engine boundary conditions or with modifications for wind tunnel measurements are very similar to the signatures of the original shapes.

1. INTRODUCTION

The mitigation of the sonic boom is essential for the development of a future low boom supersonic aircraft that is allowed to fly supersonically over land. According to current regulations like the FAR 91.817, the operation of civil supersonic aircraft is prohibited over land in most countries unless it will avoid a sonic boom to reach the surface [1].

The research to decrease the annoyance of the sonic boom for the public has a long history and was mostly required when Concorde entered service. Compared to methods used a few decades ago [2], the aerodynamic low-boom shape design can rely on high fidelity simulations today due to much improved computational resources. As a result of increasing interest and progress from industry to build and certify new supersonic airplanes, regulatory authorities are now required to define acceptable levels of the sonic boom and appropriate certification procedures. The RUMBLE (RegUlation and norM for low sonic Boom LEvels) project is funded by European Commission and aims at providing the necessary evidence and proofs supporting new regulations regarding low-level sonic boom impacts.

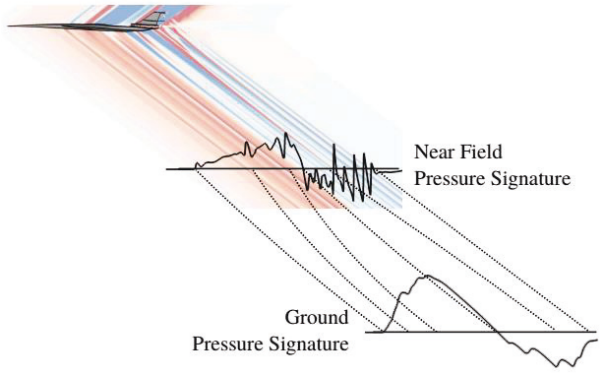

FIG 1. Numerical simulation of the sonic boom on the ground.

RUMBLE work package two focuses on the validation of numerical methods for sonic boom prediction as well as the design of low boom aircraft concepts. The state-of-the-art for the numerical simulation of the sonic boom usually consists of three steps (compare FIG 1):

- Near-field simulation with CFD (Computational Fluid Dynamics) codes up to several body lengths from the aircraft and extraction of the near-field pressure signatures.
- Calculation of the ground signatures by simulating the propagation of the pressure disturbances through the atmosphere with dedicated numerical codes.
- Estimation of the human perception by applying feasible loudness metrics.

In the context of the AIAA Sonic Boom Prediction Workshops (SBPW) [3] the German Aerospace Center (DLR) has developed a robust process to predict near-field pressure signatures of supersonic aircraft. Cross-code verifications as well as validations with experimental results have proven the accuracy of the predicted pressure signatures [4]. The numerical setup used for the SBPWs was applied and improved in RUMBLE. This paper describes the assessment of near-field TAU simulations for the geometries developed within the RUMBLE project. The propagation of the near-field signatures to the ground as well as the loudness metrics calculation is conducted by the partners.

Most of the design work for the RUMBLE shapes was performed by Airbus UK, Dassault Aviation and ONERA (Office national d'études et de recherches aérospatiales). However, DLR contributed with experience on the high fidelity design of low boom – low drag supersonic bodies [5]. In this paper the DLR design process for the fuselage is described. The front part of the fuselage was improved using a near-field target signature, whereas a parameter study was conducted for the rear part of the fuselage.

2. GEOMETRIES

The RUMBLE geometry is a single engine supersonic aircraft with large sweep angles in the inner part of the wing and a decreased sweep angle in the outer part of the wing. The design process in RUMBLE is based on an iterative exchange between overall aircraft design (OAD) and high-fidelity low boom – low drag shape design. FIG 2 shows an overview of the latest RUMBLE shape (R3).

doi:10.25967/530263

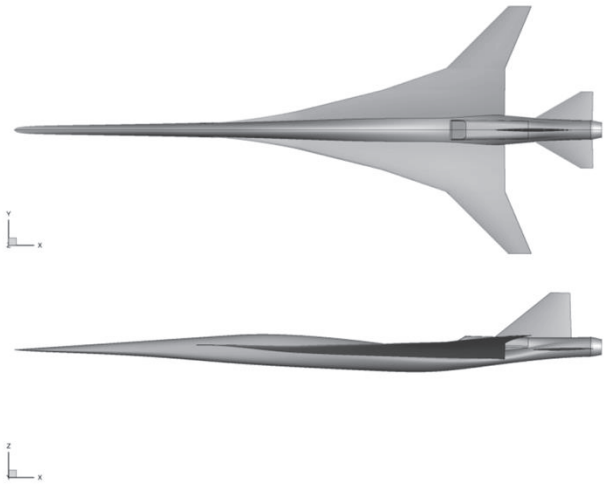

FIG 2. RUMBLE R3 geometry overview.

2.1. RUMBLE Milestone Shape Evolutions

In this paper, numerical near-field simulations for four RUMBLE milestone shape evolutions and some derivatives will be analyzed. The geometrical modifications can be summarized as follows:

- R0-1: Initial RUMBLE geometry.
- R1-1: Cross-sectional area of the fuselage decreased, length of the nose increased, wing twist improved, thickness of horizontal and vertical tail decreased.
- R2: Duck-like nose design included, wing leading edge extension (APEX) added, and fairing for landing gear added. Engine inlet moved aft.
- R3: Smoothed upper fuselage shape, improved wing and fuselage geometry, as well as modified engine inlet and horizontal tail positions.

While most simulations at DLR were performed using flow-through nacelle geometries, a simulation with powered engine boundary conditions was conducted for the R2 shape to assess the influence of the inlet compression and the plume on the numerically predicted pressure signatures. Additionally, a shape with a blocked engine inlet and a sting attached to the nozzle are derived in order to assess the influence of these modifications on the near-field pressure signatures.

2.2. Parameterization of the Geometry

A complex parametric CAD model of the fuselage has been developed based on the DLR universal aircraft model and experience from previous low boom optimizations. An overview of the final parametric model for the nose and rear fuselage design is shown in FIG 3 and FIG 4.

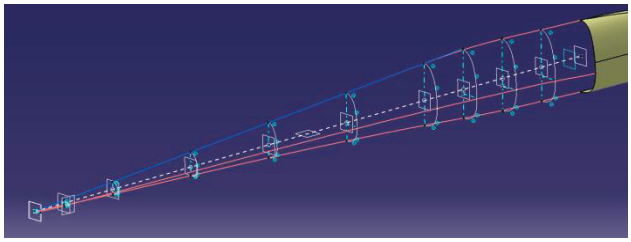

FIG 3. Parameterization of the nose.

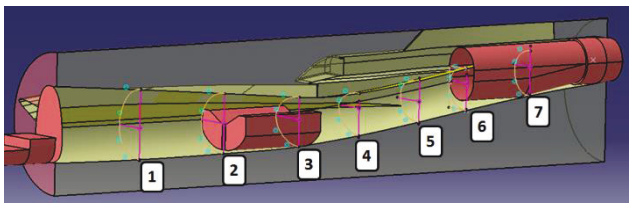

FIG 4. Parameterization of the rear fuselage including OAD constraints.

The shape of the fuselage is defined at different longitudinal sections. For the nose design, nine sections are used, while the rear fuselage design study is performed with seven cross sections. The spacing of the cross sections is large where few aircraft components are interacting and small at regions with strong interactions, e.g. the fuselage and wing leading edge junction.

FIG 5 explains the specification of the height of the fuselage by using b-splines. The positions of the section size control points are used as design parameters for the height of the fuselage. Similarly, the width of the fuselage is specified. In regions where OAD constraints have to be fulfilled, normal splines are used instead of b-splines and they are connected to the b-splines using tangency conditions.

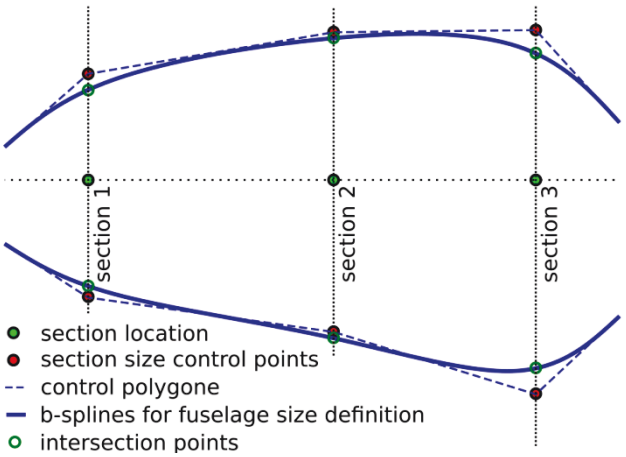

FIG 5. Schematic of the cross section sizes with two b-splines on the symmetry plane.

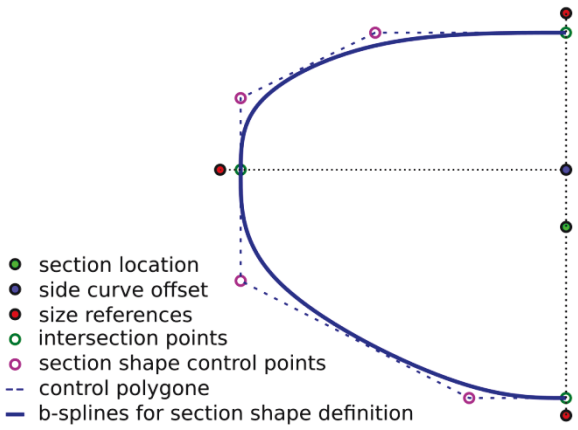

FIG 6. Schematic of the cross sectional shape parameterized using two b-splines.

The shape of the sections is defined using two b-splines – one for the upper and one for the lower part, as shown in FIG 6. The parameterization is used to shape the fuselage sections in a way that OAD constraints like the cockpit, landing gear, and engine volume are respected (see FIG 4). During the automatic design process, the size of the sections is allowed to change but the relative shape of the sections is not modified in order to limit the number of design variables to the most relevant ones. As a result, the nose design was based on 13 design parameters and the rear fuselage design was based on seven design parameters.

Intersections of the fuselage with the wing, the horizontal and vertical tail plane, as well as the nacelle were recalculated at all design iterations. This setup results in a CAD model that is very robust to strong parameter changes without producing irregular geometries but has sufficient potential to obtain differently shaped near-field pressure signatures.

The main idea for the re-design of the nose was to cause a controlled shock at the tip of the nose by increasing the width of the nose significantly (see top view in FIG 7). A similar nose shape design has been used by NASA for the C608 geometry which is a late design iteration of the NASA X-59 QueSST low-boom flight demonstrator. This geometry has been analyzed by the author in the context of the third SBPW. The motivation to create a controlled shock at the nose is to increase the duration of the pressure signature on the ground and thus decrease the loudness. The resulting shape is referred to as the “duck-like” nose shape.

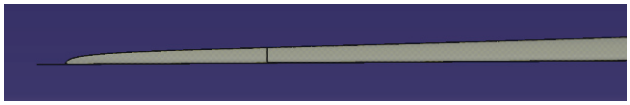

FIG 7. Duck-like nose view from top.

3. GRID GENERATION APPROACH

The grid setup is based on the best-practice of the authors described in reference [5]. In contrast to the grids for the Sonic Boom Prediction Workshops, in this case a modular grid generation approach is used. This means that only a part of the grid needs to be re-generated, which has two advantages. First, the geometries can be switched out easily during design studies. This decreases the time required to generate the grid. Second, the influence of different grids on the solution decreases.

The angle of attack at cruise is not included in the geometry or the grid. The grid deformation technique is used to change the angle of attack during the simulations according to a target lift coefficient while keeping the far-field grid aligned to the Mach cone.

FIG 8 and FIG 9 show the mixed-element grid setup of the CENTAUR [6] grids for inviscid simulations. The near-field consists of unstructured tetrahedral in the core part and the far-field is fully structured. All cells in the far-field are aligned to the free-stream Mach cone. An elliptical cross section of the inner part is used to decrease the size of unstructured and unaligned elements which reduces numerical dissipation. The grid extends to seven body lengths in radial direction. The surface resolution is sufficiently fine to prevent unphysical shocks and expansions due to the surface discretization.

The general resolution of the grid is 500 nodes in stream-wise direction next to the aircraft while the nose is refined and parts of the grid upstream of the Mach cone are increasingly coarse. The structured far-field has 100 nodes in radial direction. Cells below the geometry are uniformly distributed in circumferential direction with a 1° resolution, while the grid density decreases above the geometry. The resulting grids have around 12 million nodes.

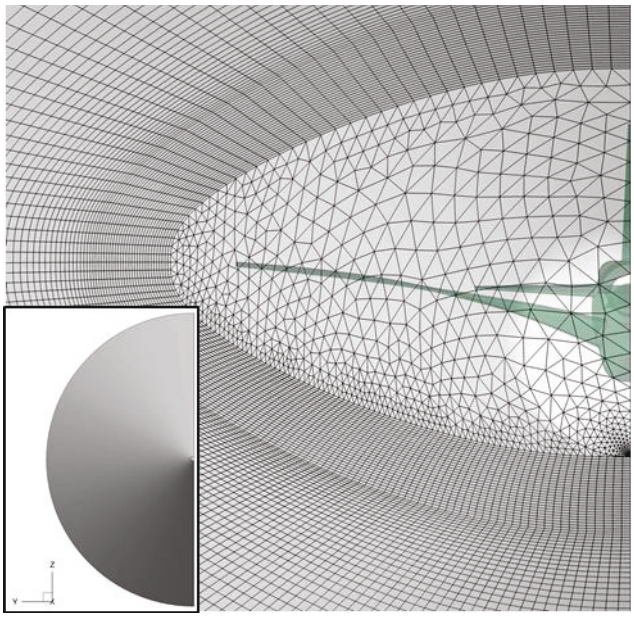

FIG 8. Front view of the grid.

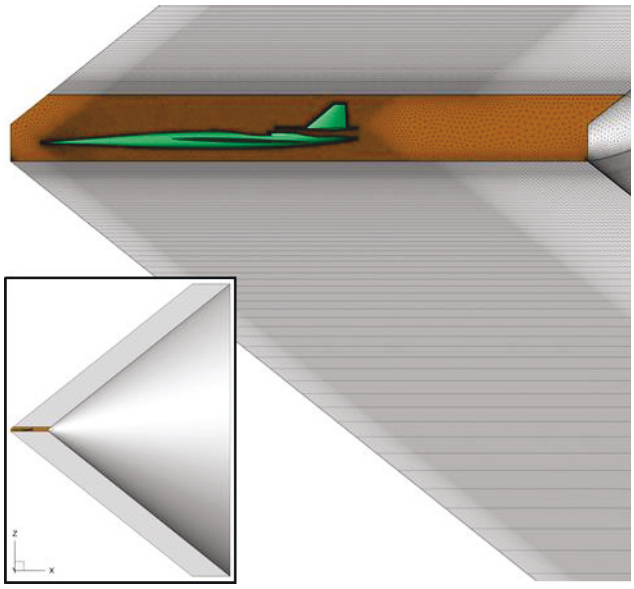

FIG 9. Symmetry plane view of the grid.

Compared to many common applications the proportion of tetrahedra is larger in grids for sonic boom near-field simulations because the shocks need to be properly resolved. As a result, a modular grid generation process has a larger potential to decrease the time required to generate the grids. Two modular grid generation setups for the nose and rear fuselage design were used, as shown in FIG 10 and FIG 11. The inner module is highlighted with blue grid lines on the symmetry plane and green grid lines for the aircraft geometry. This part of the

grid is replaced during the design process, whereas the outer (orange and black) part of the grid remains constant.

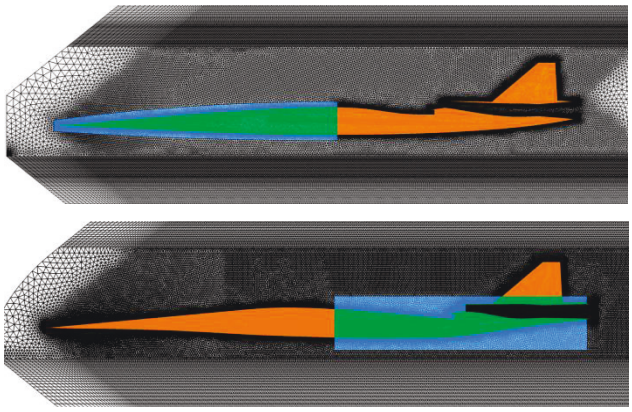

FIG 10. Modular grid generation setup for the nose (upper) and rear fuselage design (lower)

The modular grid generation process including the volume grid takes around two minutes for the nose and five minutes for the rear part of the fuselage. Comparing those values to 60 minutes in total for the generation of a grid from scratch shows a significant improvement when running design studies and confirms the potential of the modular grid generation approach for low-boom design activities.

4. NUMERICAL SETUP

The near-field CFD simulations are performed with the DLR TAU code [7], which is based on an unstructured finite-volume approach for solving the Euler or Reynolds-averaged Navier-Stokes (RANS) equations on hybrid grids. The second-order accurate AUSMDV [8] upwind scheme is applied for the spatial discretization of the convective fluxes and an implicit lower upper symmetric Gauss Seidel scheme is used for time stepping. The gradients are computed using a Green Gauss approach. The limiting strategy by Barth and Jesperson [9] with modifications proposed by Venkatakrishnan [10] is used to stabilize the numerical scheme. All calculations performed for this study are Euler simulations without multigrid acceleration. The cruise altitude is 36,000ft and the Mach number is given as M=1.6. The target lift coefficient for the cruise condition is C_L = 0.038. An automatic method for adjusting the angle of attack with grid deformation is applied to obtain the target lift coefficient [5]. The average run time of one simulation is between one and three hours.

4.1. Extraction of the Pressure Signatures

The pressure signatures are extracted and compared at several radial distances R and circumferential locations Φ. The pressure signature extraction from the 3D simulation data along the x-coordinate is shown as green line in FIG 11.

For a better comparison and understanding of the pressure signatures, the distance from the nose in freestream direction X is normalized by the Mach angle μ and the body length L. Pressure amplitudes of axisymmetric wave fields decrease with the square root of distance R from the aircraft [11]. At a sufficient distance from the aircraft the wave field can be treated as locally axisymmetric, so the pressure signatures and mid-field pressure contours in this paper are normalized by the square root of the relative distance to the aircraft R/L.

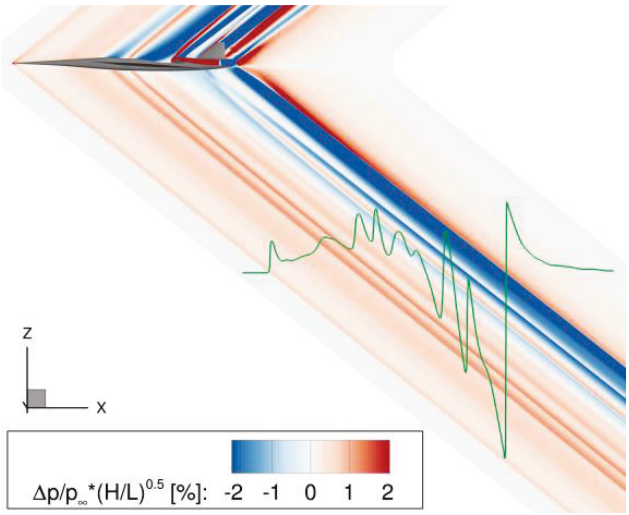

FIG 11. Symmetry plane pressure contour and extraction of the on-track pressure signature at one body length distance (R/L=1)

4.2. Nose-Shape Design Process Setup

In order to decrease the loudness of the sonic boom, the parametric CAD model and the modular grid generation were integrated into a surrogate-based multi-objective optimization process. For that, the Powerful Optimization Tools with Surrogate Modeling (POT) were used. They have been developed at DLR [12], [13]. Within RUMBLE the framework is used to run designs of experiments (DoE), create surrogate models and optimize the aerodynamic shape of the RUMBLE configuration. The framework provides various algorithms to build surrogate models for single and multi-objective optimizations and possibilities to tune the hyperparameters of Kriging surrogate models. It offers an interface to run the iterations for the DoE in parallel, which significantly decreases the time required to run the optimization.

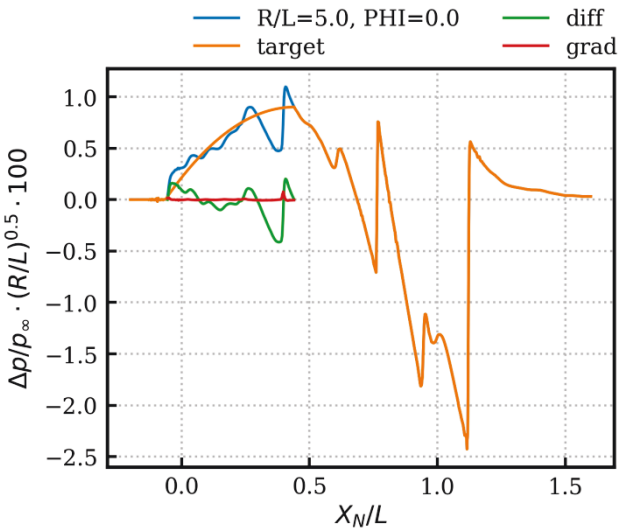

FIG 12. Near-field objective function for the optimization of the nose

For the optimization of the nose an objective function based on a target near-field signature with a smooth compression for X_N/L =0.46 was defined, as shown in FIG 12. The objective was formulated to minimize the area between the current (blue line) and the target pressure signature (orange line). Additionally, a penalty for large pressure derivatives was added (red line) in order to avoid strong oscillations in the geometry.

All near-field pressure signatures obtained through the optimization were propagated by Dassault Aviation using their propagation tool and loudness metrics DAbang. The results showed that the optimization was able to decrease the loudness of the sonic boom. However, within the design of experiments there were even more favorable configurations with oscillating near-field signatures where the compression and expansion waves interacted while propagating through the atmosphere. In some cases this was beneficial for the sonic boom loudness on the ground. As a result, the nose shape of the configuration with the lowest loudness after propagation was selected for the R2 configuration instead of the shape obtained with the target near-field signature.

5. NEAR-FIELD SIMULATION RESULTS

In this section, the RUBMLE shape evolutions and their derivatives described in section 2.1 are analyzed numerically.

5.1. Simulations for the Shape Evolutions

FIG 13 and FIG 14 show the near-field pressure signatures for the on-track and 30° off-track angles at three body lengths distance. The corresponding symmetry plane pressure contours for the RUMBLE shapes with flow-through nacelle are shown in FIG 15.

The initial geometry (R0-1) has a blunt nose which causes a strong shock. Due to the magnitude of this shock it will cause a loud sonic boom on the ground. An improved design (R1-1) included first top level aircraft requirements. Additionally, the magnitude of the nose shock has been reduced significantly by increasing the length of the nose as well as decreasing the cross-sectional area of the fuselage. This can clearly be seen in the symmetry plane contours and the near-field pressure signature, where the gradient of the initial compression at the nose has been reduced from R0-1 to R1-1 and the maximum overpressure could be decreased.

In order to further reduce the loudness and increase the efficiency of the aircraft, the R2 shape included the low-boom “duck-like” nose shape design and a low-drag optimized wing. However, the R2 near-field is mostly influenced by the landing gear fairing which causes a strong compression and following expansion below the aircraft. As a result, the maximum overpressure increases significantly. The pressure signature in the rear part of the aircraft changes slightly due to the different fuselage shapes but the general compression and expansion pattern remains similar.

The R3 shape has the same nose shape as the R2 shape, so the pressure signature in the front part is identical. However, due to an improved fuselage area ruling, the maximum overpressure was decreased by the partners. The modified inlet and HTP positions cause a different interaction of the compression and expansion waves in the rear part of the aircraft. An additional compression wave at X_N/L =0.9 occurs due to interaction of the inlet shock with the wing trailing edge and the HTP leading edge. Furthermore, the magnitude of the final compression at X_N/L =1.1 is decreased which also means that the minimal pressure no longer occurs just before the final compression.

Comparing the on-track pressure signatures with the off-track pressure signatures for all shape evolutions, the off-track pressure signatures at the rear part of the aircraft are less influenced by geometrical changes. Also, the off-track pressure signatures are less influenced by the shape of the components but mostly by their arrangement.

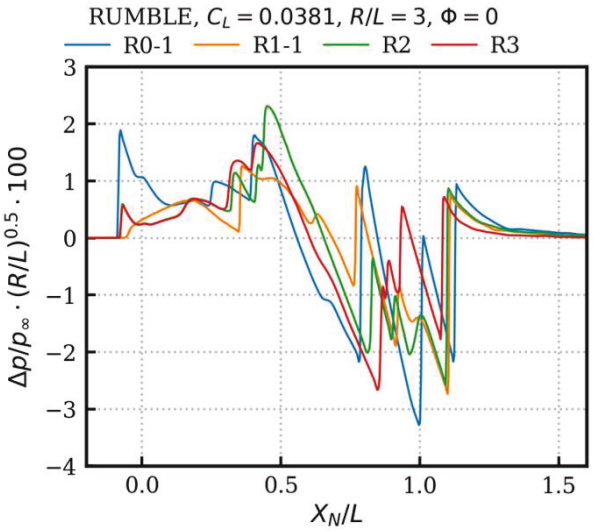

FIG 13. On-track pressure signatures at three body lengths distance for different RUMBLE shape evolutions.

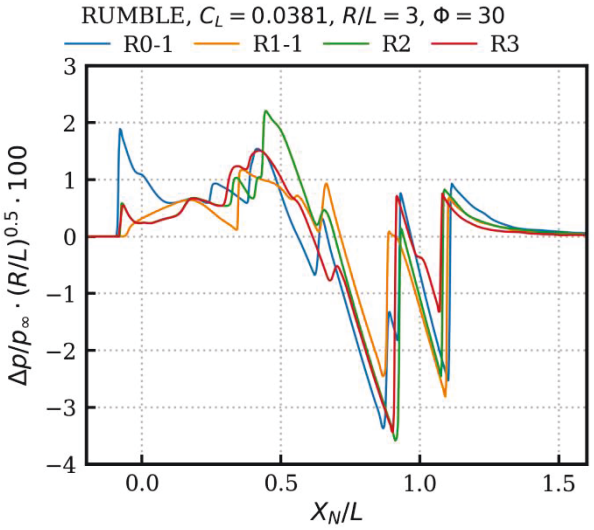

FIG 14. 30° Off-track pressure signatures at three body lengths distance for different RUMBLE shape evolutions.

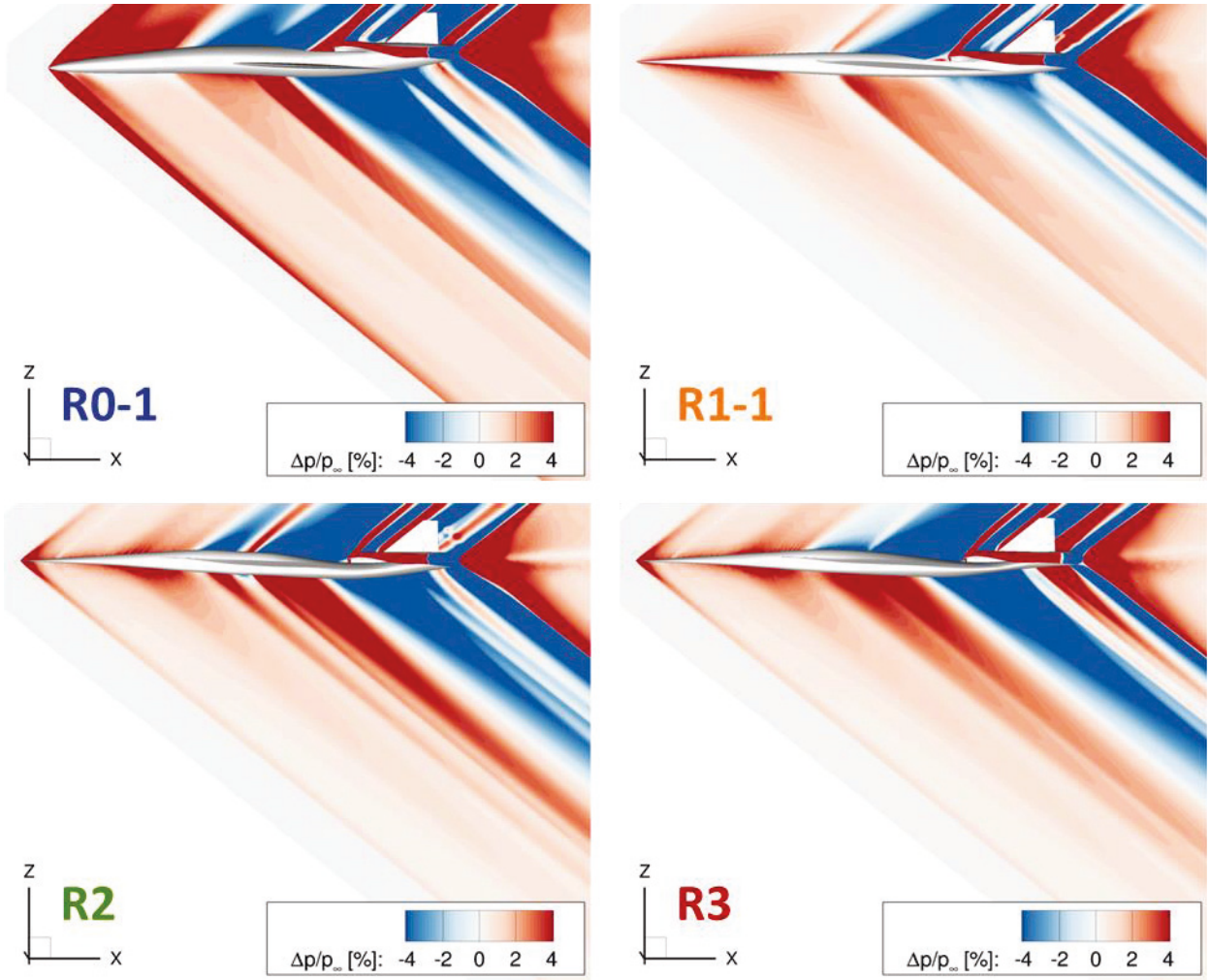

FIG 15. Symmetry plane pressure contours for different RUMBLE shape evolutions.

5.1.1. Improved Nose Shape Design

The design of the nose shape was based on the R1-1 geometry and the improved nose shape (R1-XAD) as well as the wing leading edge extension (APEX) were included in the R2 geometry. For a better comparison of the two cases, the result of the design process is summarized in FIG 16.

While the R1-1 was designed to have a smooth compression at the nose, the R1-XAD improved design features a relatively strong shock at the tip of the nose. This shock is directly followed by an expansion to nearly ambient pressure. Except for the nose shock, the compression up to X_N/L =0.25 is relatively smooth.

For the R1-1 geometry the wing leading edge shock was interacting with the cockpit volume, thus causing a strong compression around X_N/L =0.4. In contrast to this, the R1-XAD was shaped so that it will generate several compressions and expansions in this part of the pressure signature. Because the compression due to the wing leading edge and lift contribution will always have a strong gradient, this approach has shown to be the best way to decrease the loudness on the ground. For the provided cruise altitude these oscillations in the near-field pressure signatures interact during the propagation and result in a smooth ground signature with a quieter sonic boom.

Although the nose is not axisymmetric the influence of lift is small in this part of the aircraft and the features in the off-track pressure signatures are very similar to the on-track signatures in both shape and magnitude (compare also FIG 13 and FIG 14).

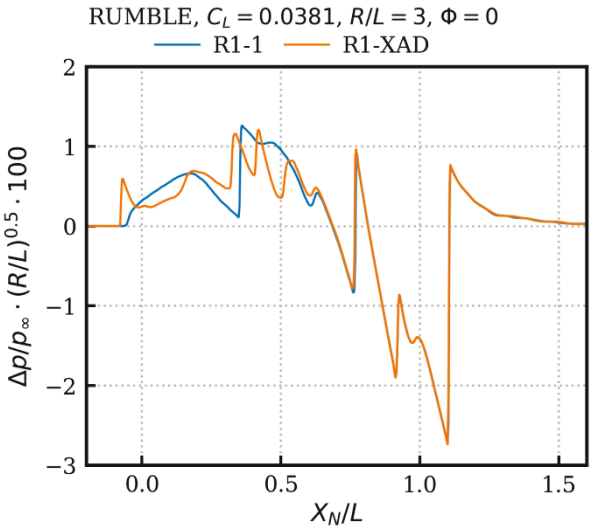

FIG 16. Near-field signature of improved nose design.

5.1.2. Understanding the Pressure Signature

Matching features visible in the near-field pressure signatures to the geometrical components of the aircraft can be difficult due to complex three-dimensional interactions of multiple components, especially in the rear part of the aircraft. FIG 17 gives an overview of the pressure signature of the R3 shape and the corresponding geometrical features. The volume added by the main landing gear (MLG) fairing has a significant influence on the pressure field.

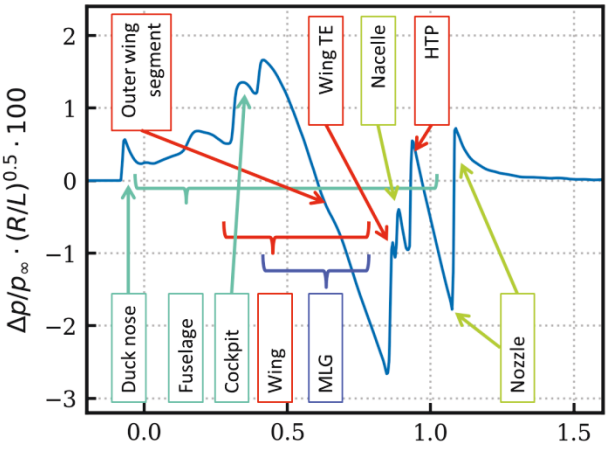

FIG 17. Matching features visible in the near-field pressure signature to geometrical components of the R3 geometry.

5.2. Influence of Powered Engine Boundary Conditions

Although most simulations were performed using a flow-through nacelle geometry, an engine model has been applied for the R2 geometry in order to verify the simplified approach. The results for the simulations are shown in FIG 18. The difference between the powered case and the flow-through nacelle are minor.

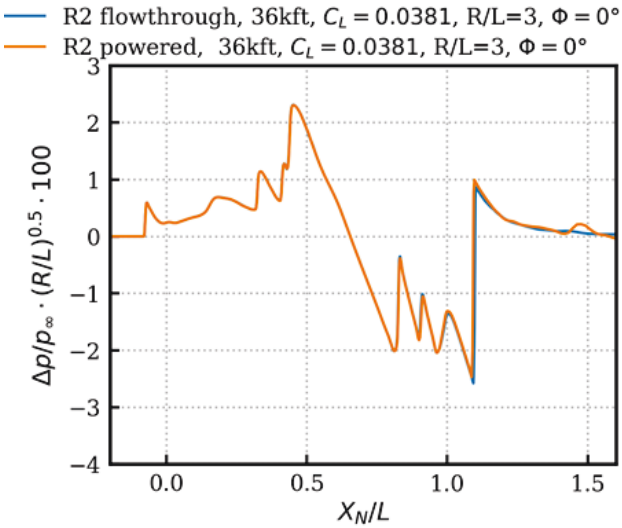

FIG 18. Comparison of the pressure signatures for flow-through nacelle and powered engine boundary conditions

The oscillation that can be observed at X_N/L =1.5 is not physical but a numerical artifact. The grid setup for both simulations was nearly identical to reduce the grid influence. However, this means that the grid for the engine plume is not refined further away from the aircraft. The oscillations in the near-field pressure signatures occur due to the grid becoming coarser around X_N/L =1.5 which creates numerical dissipation in the engine plume.

5.3. Wind Tunnel Shape Study

In preparation for the RUMBLE wind tunnel test, a numerical study has been performed to assess feasible simplifications of the R3 geometry that allow the manufacturing of a scaled wind tunnel model. It was decided to close the inlet at the lip of the nacelle and attach the sting at the nozzle.

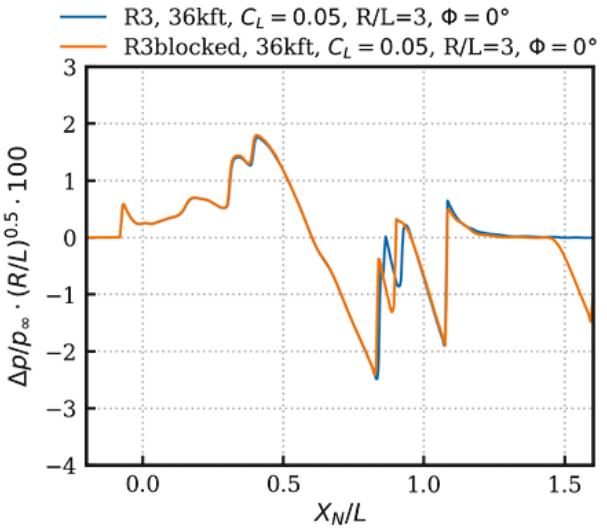

FIG 19. Influence of the blocked inlet and sting on the near-field pressure signature (on-track).

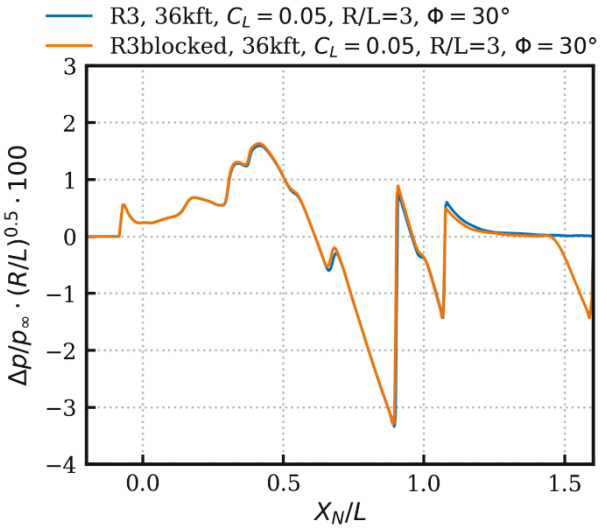

FIG 20. Influence of the blocked inlet and sting on the near-field pressure signature (30° off-track).

As shown in FIG 19 the influence of the geometrical modifications on the on-track pressure signatures is small. The magnitude of the inlet shock increases and the pattern merges with the wing trailing edge oscillation. The strong expansion starting at X_N/L =1.5 is caused by the

selected shape of the sting. The influence of the blocked inlet on the off-track pressure signatures is minor, as shown in FIG 20.

5.4. Influence of the Angle of Attack

The lift coefficient required for a trimmed flight varies with aircraft mass and flight altitude. Pressure signatures are strongly influenced by the local lift distribution below the aircraft. Because of the numerical effort required to design low-boom shapes, the process will often focus on the cruise flight condition today. Thus, the loudness can increase significantly if the local lift distribution changes. FIG 21 shows the near-field pressure signatures for the R3 shape at different lift coefficients. As expected, the maximum overpressure and the minimal pressure increase with increased lift coefficients.

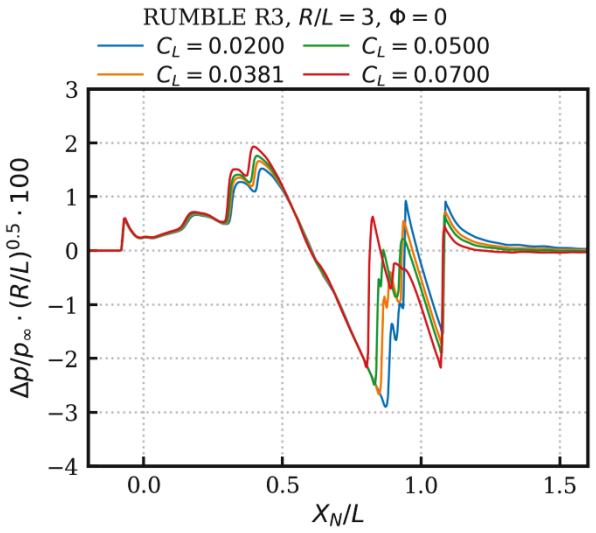

FIG 21. Influence of the lift coefficient and angle of attack on the near-field pressure signature.

5.5. Rear Fuselage Design Study

The loudness of the RUMBLE shapes is mostly driven by the rear part of the aircraft. In order to further reduce the loudness, a design study for the rear fuselage shape has been performed.

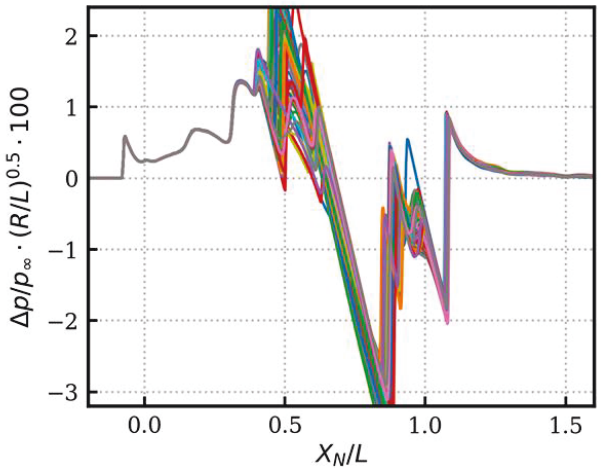

FIG 22. Near-field pressure signatures for varying rear fuselage geometries.

FIG 22 shows the near-field pressure signatures for all design iterations that were simulated based on the parametric fuselage model. Although the chosen parameter space is large, the terminating shock is not influenced by the fuselage design at all. In order to reduce the terminating shock, a different nozzle design has to be applied. However, the vertical tail plane also influences the rear part of the pressure signature. Moving the VTP forward will also have a positive effect on the loudness but will have a negative influence on the stability of the aircraft.

Additionally, the influence of the rear fuselage design on the gradient of the main expansion is minor and the influence on the position of the expansion is small.

6. SUMMARY AND OUTLOOK

In this paper, an accurate process to calculate pressure signatures of low boom aircraft with the DLR TAU code was described and applied for the RUMBLE milestone shapes. A low-boom design process for the nose and the rear part of the fuselage was presented with a focus on a robust parameterization of the fuselage geometry using a combination of splines and b-splines to account for geometrical constraints.

The simulations showed that a smooth target near-field signature can lead to a quieter sonic boom. However, this method is not able to find configurations with oscillations in the near-field pressure signature that might be beneficial for the shape of the ground signature and the loudness of the aircraft. For realistic aircraft geometries the propagation and loudness metrics should be included in the low boom optimization process to be able to resolve the interaction of oscillating near-field pressure signatures.

Comparing a flow-through nacelle to powered boundary conditions, the influence of the engine model on the pressure signatures is minor.

The pressure signature of a wind tunnel shape derivative with a blocked engine inlet and a sting attached to the nozzle did not significantly change. Thus, this approach was found to be feasible to simplify the manufacturing of scaled wind tunnel models for validation purposes.

A parameter study with different rear fuselage geometries showed that the terminating compression of the pressure signature is mostly influenced by the nozzle shape. This experience will be used in future studies to further improve the rear fuselage and nozzle shape and decrease the loudness of the RUMBLE shape.

ACKNOWLEDGEMENTS

The research leading to these results has received funding from the European Union's Horizon 2020 research and innovation programme under grant agreement No 769896.

The design of the RUMBLE shapes described in this paper was mostly performed by Olivier Atinault, Gérald Carrier, Pierre-Elie Normand, Stephen Powell and Stephen Rolston, which is gratefully acknowledged by the author. Additionally, the author would like to thank Pierre-Elie Normand for propagating the near-field signatures to the ground and calculating the loudness metrics.

Furthermore, the author wishes to thank Gunther Wilke for the development of the POT framework and for helping out with any questions concerning the setup of the optimization process.

REFERENCES

[1] “Civil aircraft sonic boom,” Code of Federal Regulations, Title 14, Part 91, Section 817, 2017.

[2] Seebass, R., and Argrow, B., “Sonic Boom Minimization Revisited,” AIAA Paper 1998–2956, Jun. 1998. doi:10.2514/6.1998-2956.

[3] Park, M. A., and Nemec, M., “Near Field Summary and Statistical Analysis of the Second AIAA Sonic Boom Prediction Workshop,” AIAA Paper 2017-3256, Jun. 2017. doi:10.2514/6.2017-3256.

[4] Kirz, J., and Rudnik, R., “DLR Simulations of the First AIAA Sonic Boom Prediction Workshop Cases,” AIAA Paper 2017-0276, Jan. 2017. doi:10.2514/6.2017-0276.

[5] Kirz, J., “Surrogate Based Shape Optimization of a Low Boom Fuselage Wing Configuration,” AIAA Paper 2019–3489, Jun. 2019. doi:10.2514/6.2019-3489.

[6] CentaurSoft, “CENTAUR - Mesh (Grid) Generation for CFD and Computational Simulations,” 2016. www.centaursoft.com [accessed 01 Dec. 2016].

[7] Schwamborn, D., Gerhold, T., and Heinrich, R., “The DLR TAU-Code: Recent Applications in Research and Industry,” 2006. ECCOMAS CFD 2006: European Conference on Computational Fluid Dynamics.

[8] Wada, Y., and Liou, M.-S., “An accurate and robust flux splitting scheme for shock and contact discontinuities,” SIAM Journal on Scientific Computing, Vol. 18, No. 3, 1997, pp. 633–657. doi:10.1137/S1064827595287626.

[9] Barth, T., and Jesperson, D., “The Design and Application of Upwind Schemes on Unstructured Meshes,” AIAA Paper 1989–0366, Jan. 1989. doi:10.2514/6.1989-366

[10] Venkatakrishnan, V., “On the Accuracy of Limiters and Convergence to Steady State Solutions,” AIAA Paper 1993–880, Jan. 1993. doi:10.2514/6.1993-880.

[11] Plotkin, K., “Review of Sonic Boom Theory,” AIAA Paper 1989–1105, Apr. 1989. doi:10.2514/6.1989-1105.

[12] Wilke, G. A., “Variable-Fidelity Methodology for the Aerodynamic Optimization of Helicopter Rotors,” AIAA Journal, 2019, pp. 1–14. doi:10.2514/1.J056486.

[13] Wilke, G. A., “Aerodynamic Optimization of Helicopter Rotor Blades using Variable Fidelity Methods,” Ph.D. thesis, Technische Universität Carolo-Wilhelmina zu Braunschweig, November 2017.